A stable method to model the acoustic response of multilayered structures

O. Dazel, J.-P. Groby, B. Brouard, and C. Potel

Citation: J. Appl. Phys. **113**, 083506 (2013); doi: 10.1063/1.4790629
View online: http://dx.doi.org/10.1063/1.4790629
View Table of Contents: http://jap.aip.org/resource/1/JAPIAU/v113/i8
Published by the American Institute of Physics.

A stable method to model the acoustic response of multilayered structures

O. Dazel,[a] J.-P. Groby, B. Brouard, and C. Potel
Laboratoire d'Acoustique de l'Université du Maine—UMR CNRS 6613, Avenue Olivier Messiaen, F-72 085 Le Mans Cedex, France

(Received 25 June 2012; accepted 23 January 2013; published online 25 February 2013)

A general approach to determine the acoustic reflection and transmission coefficients of multilayered panels is proposed in this paper. Contrary to the Transfer Matrix Method (TMM), this method does not become unstable for high frequencies or large layer thicknesses. This method is shown to be as general as the TMM and mathematically equivalent. Its principle is to consider a so called Information Vector which contains all the information necessary to deduce the State Vector through a Translation Matrix. The Information Vector is of reduced length compared to that of the State Vector and can be propagated in any layer without involving exponentially growing terms. In addition, this method enables the coupling between any type of physical media as far as proper boundary relations can be written. Moreover, the method does not lead to an enlargement of the systems' size in the case of interfaces between media of different physical type. Finally, this method can be easily implemented in numerical codes. The method is validated on three cases classically encountered in acoustic problems. However, it is general enough to model any type of multilayered problems in any field of applied physics. © *2013 American Institute of Physics*. [http://dx.doi.org/10.1063/1.4790629]

I. INTRODUCTION

The Thomson-Haskell method[7,8,12–15,20–22] also known as the Transfer Matrix Method (TMM) is often used in various domains of physical modelling (in acoustics to model sound packages or composite materials, in electromagnetism, in geodynamics, etc). This method computes the response of planar multilayered systems presented in Fig. 1. Each layer is of infinite extent in the lateral directions and the structure is excited by an incident monochromatic plane wave. Basically, the method consists in decomposing the wave fields in each layer into forward and backward waves and in applying the boundary conditions at each layer interfaces. This method is very convenient because of its flexibility: the propagation in a layer is performed with matrix multiplication and media of different physical types (solids, fluids, viscoelastic and poroelastic materials, etc) can be coupled through interface matrices. The TMM is also shown to be fast. For structures with invariance by rotation around the thickness direction, a Cartesian coordinate system can be attached to the configuration such that the polarization of the wave is in the incident plane. Boundary relations, leading to Snell-Descartes laws, show that the propagation is in the same plane as the incident wave thereby reducing the 3D problem to a 2D one.

The principle of the TMM is to consider a State Vector, whose components depend on the position along the layer thickness. For example, in mechanical applications, this vector merges the particle displacements with the stresses applied on a surface perpendicular to the thickness of the sample. The Transfer Matrix of a layer provides linear relations between the values of the State Vector on each sides of the layer. It can be shown that, for a given layer, the length of this vector is equal to the number of the waves (both forward and backward waves being considered). As the number of waves depends on the physical nature of the medium in the layer, a natural consequence is that the length of the State Vector is not always constant along the thickness of a multilayered structure when it consists of different types of media. Consequently, the TMM is, theoretically, a general method to predict reflection and transmission coefficient of multilayered structures. It has been applied successfully in a huge number of cases, see, for example, Refs. 1–3, 8, 12, and 14. Extensions have also been proposed, for example, to take the finite size effects of panels into account.[18]

Even though the method is exact from a mathematical point of view, divergences can occur in its results. It is especially the case for high frequencies and/or large layer thicknesses. The reason of this divergence is a bad numerical evaluation of the involved exponential terms by finite-arithmetics computers. This is a classical and well known numerical problem which has been observed by several authors in many fields of physics[4,9,16,17,19] and some

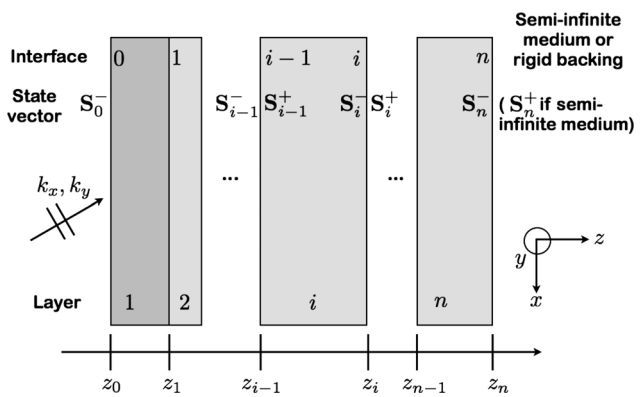

FIG. 1. Panel composed of n layers.

[a]olivier.dazel@univ-lemans.fr.

strategies have been proposed to avoid this problem. Nevertheless, none of the proposed techniques was shown to be both sufficiently general to model all kinds of problem and simple enough to be implemented without a prohibiting cost. For example, most of the techniques proposed in geomechanics[9,17] and for the ultrasonic propagation in composite materials[4,19] concerns transmission problems composed of layers of analog physical medium and no example is found in the literature of a stable technique that can be applied to rigid backing problems.

Among the above techniques, one particular category of methods[10,19,23,24] strongly inspire the authors. They are based on recursive approaches. In 1997, Yang proposed a spectral recursive method to model electromagnetic waves in generalized anisotropic layered media.[24] Even if this technique was only devoted to a single type of medium and applied to a transmission problem, it can be extended and generalized. This is the purpose of the present paper. Hence, a stable numerical method is developed and proposed to model wave propagation in multilayered structures. Contrary to the TMM approach, the principle of the present approach is not to propagate the whole State Vector in a layer; only the non redundant information is propagated. One key point is that this method is mathematically equivalent to the TMM and can thereby be considered as exact.

Section II introduces the configuration of interest and the notations used in the present work. Section III presents the method from an abstract point of view. These two sections illustrate the generality of the approach. In order to help the reader to understand the approach, examples are also given in these two sections. These ones are associated with the application cases presented in Sec. IV.

II. CONFIGURATION OF INTEREST

In this work, multilayered panels as in Fig. 1 are considered. A Cartesian $\{x, y, z\}$ coordinate-system is used. The panel is assumed to be infinite along the x and y axis. The z axis corresponds to the thickness direction. The different layers of the panel can be associated with several types of medium encountered in mechanics (elastic or viscoelastic solids, fluid media— air or any gas, equivalent fluid model, limp model—, isotropic or transverse isotropic poroelastic material…). However the proposed method is sufficiently general to be adapted to piezoelectric materials or to electromagnetic media. Each layer is assumed homogeneous (i.e., with constant physical properties). Concerning excitation, a monochromatic (angular frequency ω and convention $e^{j\omega t}$ with $j=\sqrt{-1}$) plane wave with a $\{x,z\}$ wave number denoted by $\{k_x, k_y\}$ is considered. In this paper, $[\mathbf{I}_\nu]$ denotes the identity matrix of size ν. Even if it is not considered in this work, the proposed technique can be applied in the case of diffuse field excitation without restriction by the classical angular integration or to lineic sources through a spatial Fourier Transform. If the panel is supposed to be invariant by rotation around the z-axis, the polarization of the incident plane wave can be considered to be in the $\{x, z\}$ plane and the wave number component in the y direction k_y is equal to zero. Hence, in this case, k_x is given by

$$k_x = k_0 \sin(\theta), \tag{1}$$

for all the layers where k_0 is the wave number in the incident medium and θ is the incident angle. This 2D assumption will be considered in the examples of Sec. IV but is not necessary in the general case presented in Sec. III. Two termination conditions can be considered on the right-hand side of the structure: it can be bounded by a rigid wall or waves are radiated into a semi-infinite medium.

Let n be the number of layers in the panel. They are then separated by $n+1$ interfaces which are labelled from 0 to n; interface 0 is the one with the incident medium and interface n is associated to the termination. Hence, layer i is limited by interfaces $i-1$ and i. Each interface is determined by its coordinate z_i, $i \in \{0..n\}$ and the thickness of layer i is $d_i = z_i - z_{i-1}$. Finally let $2m_i$ denote the number of waves in the layer.

For each layer, a State Vector (denoted by $\mathbf{S}(z)$) is considered. We are mostly interested in the evaluation of this vector at the interfaces of the multilayer panel. Hence, one defines:

$$\mathbf{S}_i^+ = \lim_{z \to z_i^+} \mathbf{S}(z), \quad \mathbf{S}_i^- = \lim_{z \to z_i^-} \mathbf{S}(z). \tag{2}$$

We can notice that $\mathbf{S}_n^+$ is only defined in the case of a transmission problem. Examples of State Vector, associated to the cases presented in Sec. IV, are given in Table I. u refers to displacements and σ to stresses; indices denote directions. For poroelastic materials (PEM), fields are associated with the stress decoupled formulation.[6] Note that an adequate choice of the State Vector of a layer consists in using components that are continuous fields at the interfaces.

For a given layer (i) with constant physical properties, the length of the State Vector is equal to the number $2m_i$ of waves. The Transfer Matrix $[\mathbf{M}_i]$ is deduced from the linear application which associates the values of the components of the State Vector at both sides of the layer. $[\mathbf{M}_i]$ is thus a $\{2m_i \times 2m_i\}$ matrix:

$$\mathbf{S}_{i-1}^+ = [\mathbf{M}_i]\mathbf{S}_i^-. \tag{3}$$

The expression for $[\mathbf{M}_i]$ can be obtained for example with the Stroh formalism: the State Vector can be shown to be the solution of a first order partial derivative equation:

$$\frac{\partial \mathbf{S}(z)}{\partial z} = -[\boldsymbol{\alpha}_i]\mathbf{S}(z), \quad z_{i-1} < z < z_i. \tag{4}$$

As $[\boldsymbol{\alpha}_i]$ is constant in the layer, $[\mathbf{M}_i]$ can be formally written with a matrix exponential:

TABLE I. State Vectors associated to different kinds of media.

Medium	State Vector	Medium	State Vector	Medium	State Vector
Fluid	$\left\{\begin{array}{c} u_z \\ \hline p \end{array}\right\}$	Isotropic solid	$\left\{\begin{array}{c} \sigma_{xz} \\ u_z \\ \hline \sigma_{zz} \\ u_x \end{array}\right\}$	PEM	$\left\{\begin{array}{c} \hat{\sigma}_{xz} \\ u_z^s \\ u_z^t \\ \hline \hat{\sigma}_{zz} \\ p \\ u_x^s \end{array}\right\}$

$$[\mathbf{M}_i] = \exp([\boldsymbol{\alpha}_i]d_i). \tag{5}$$

A more convenient expression can be written with a preliminary diagonalization of $[\boldsymbol{\alpha}_i] = [\boldsymbol{\Phi}_i][\boldsymbol{\lambda}_i][\boldsymbol{\Phi}_i]^{-1}$, where $[\boldsymbol{\Phi}_i]$ is the matrix of eigenvectors and $[\boldsymbol{\lambda}_i]$ the diagonal matrix of the eigenvalues of $[\boldsymbol{\alpha}_i]$. Equation (5) is now rewritten as:

$$[\mathbf{M}_i] = [\boldsymbol{\Phi}_i][\exp(\boldsymbol{\lambda}_i d_i)][\boldsymbol{\Phi}_i]^{-1}. \tag{6}$$

The diagonalization of $[\boldsymbol{\alpha}_i]$ is straightforward if one considers the expression of the State Vector $\mathbf{S}(z)$ as a function of the amplitudes $\mathbf{q}$ of the $2m_i$ waves in the layer:

$$\mathbf{S}(z) = [\mathbf{A}_i(z)]\mathbf{q}, \quad [\mathbf{A}_i(z)] = [\mathbf{A}_i(z_i)][\boldsymbol{\Delta}_i(z)], \tag{7}$$

where $[\boldsymbol{\Delta}_i(z)]$ is the diagonal matrix whose n^{th} term is equal to $\exp(jk_z(n)(z - z_i))$ where $k_z(n)$ is the wave number along the z direction associated with the n^{th} wave. The Transfer Matrix can be rewritten as

$$[\mathbf{M}_i] = [\mathbf{A}_i(z_{i-1})][\mathbf{A}_i(z_i)]^{-1} = [\mathbf{A}_i(z_i)][\boldsymbol{\Delta}_i(z_{i-1})][\mathbf{A}_i(z_i)]^{-1}. \tag{8}$$

A direct comparison of expressions (6) and (8) indicates that $[\boldsymbol{\lambda}_i]/j$ is the diagonal matrix of z–component of the wave vector and that $[\boldsymbol{\Phi}_i] = [\mathbf{A}_i(z_i)]$. Note that for the given layer, the z–origin can be chosen equal to z_i so that $[\mathbf{A}_i(z_i)]$ does not involve exponential terms. Examples and explicit expressions for $[\boldsymbol{\alpha}_i]$, $[\boldsymbol{\Phi}_i]$ and $[\boldsymbol{\lambda}_i]$ are given in Appendix A for the media considered in Sec. IV.

In the case of multilayered structures composed of several materials of the same physical type and with an adequate choice of components for the State Vector (i.e. associated to continuous fields), the global Transfer Matrix is obtained by matrix multiplication. Reflection and transmission coefficients are deduced from the global matrices. In the case of a panel composed of several types of media, it is not always possible to directly exhibit a Transfer Matrix, but it was shown possible to consider a global linear system which is deduced from both boundary relations and individual Transfer Matrices. This system is generally of larger size and its numerical implementation is not straightforward. The procedure is presented, for example, in Ref. 3 and detailed in Ref. 1 to which the reader can refer for further details.

III. PROPOSED APPROACH TO MODEL MULTILAYERED STRUCTURES

A. General overview of the proposed method

The general idea of the proposed method is to rewrite the State Vector as:

$$\mathbf{S}_i^{\pm} = [\boldsymbol{\Omega}_i^{\pm}]\mathbf{X}_i^{\pm}, \tag{9}$$

wherein $\mathbf{X}_i^{\pm}$ is thus called Information Vector. Its components can correspond either to physical fields or any combination of them which can be adequately chosen. Regardless of the significance of the components of this vector, an important aspect is that the State Vector can always be deduced from it. That is the reason why another quantity $[\boldsymbol{\Omega}_i^{\pm}]$, called Translation matrix, needs also to be determined so as to link the State and the Information Vectors. The method will then consist in an initialization step and two steps in case of rigidly bounded problems. For transmission in a semi-infinite medium problem, a third step needs to be considered.

TABLE II. Translation matrices at interface n for a fluid.

Fluid on a rigid backing	Transmission in a semi-infinite fluid
$[\boldsymbol{\Omega}_n^-] = \begin{bmatrix} 0 \\ 1 \end{bmatrix}$, $[\mathbf{X}_n^-] = \{p(z_n)\}$	$[\boldsymbol{\Omega}_n^+] = \begin{bmatrix} -\frac{\cos(\theta)}{j\omega Z_0} \\ 1 \end{bmatrix}$, $[\mathbf{X}_n^+] = \{T\}$

Step 0 (initialization) consists in determining the Translation Matrix associated with the termination condition. The two different cases should be individually considered. For the rigid backing configuration, all displacements are equal to zero, the only unknowns are the normal stresses; these stresses are the components of $\mathbf{X}_n^-$. $[\boldsymbol{\Omega}_n^-]$ is then a Boolean matrix, whose expression is straightforward. For the transmission problem, $\mathbf{X}_n^+$ corresponds to the transmission coefficients in the semi-infinite medium and $[\boldsymbol{\Omega}_n^-]$ follows from the expressions of stresses and displacements in terms of these amplitudes. The expressions for Translation matrices are given in Table II for the case of a fluid (considered in the examples of Sec. IV).

Step 1 consists in determining the value of $[\boldsymbol{\Omega}_0^-]$ which is deduced successively from the Translation Matrix $[\boldsymbol{\Omega}_n^{\pm}]$ at the termination interface. Each interface is considered in a decreasing manner. Note that values of the Information Vectors remain unknown for the moment.

Step 2 consists in finding $[\mathbf{X}_0^-]$. The State Vector in the incident medium $\mathbf{S}_0^-$ can then be written on two different forms. The first one is by Eq. (9) in which $[\boldsymbol{\Omega}_0^-]$ is deduced from Step 1. The second form is derived from the expression of the field in the incident medium written from the excitation and the unknown reflection coefficient which gives

$$\mathbf{S}_0^- = [\boldsymbol{\Omega}_0^-]\mathbf{X}_0^- = [\boldsymbol{\Omega}_0]\mathbf{R} + \mathbf{E}_0. \tag{10}$$

$\mathbf{E}_0$ corresponds to the excitation and $\mathbf{R}$ is the unknown vector of reflection coefficients. Expressions for $[\boldsymbol{\Omega}_0]$ and $\mathbf{E}_0$ are given in Table III for a illustration. Since Eq. (10) is a linear problem in $\mathbf{R}$ and $\mathbf{X}_0^-$, the unknowns are derived from:

$$\begin{Bmatrix} \mathbf{X}_0^- \\ \mathbf{R} \end{Bmatrix} = [[\boldsymbol{\Omega}_0^-]| - [\boldsymbol{\Omega}_0]]^{-1}\mathbf{E}_0. \tag{11}$$

For rigid backing configurations where $\mathbf{R}$ is the only unknown, this is the final step. For transmission problems, an additional (third) step is needed. It consists in deducing the

TABLE III. Expressions of $[\boldsymbol{\Omega}_0]$ and $\mathbf{E}_0$ for a fluid of specific impedance Z_0 and for an incident plane wave with angle θ and angular frequency ω.

$[\boldsymbol{\Omega}_0]$	$\mathbf{E}_0$
$\begin{bmatrix} \frac{\cos(\theta)}{j\omega Z_0} \\ 1 \end{bmatrix}$	$\begin{Bmatrix} -\frac{\cos(\theta)}{j\omega Z_0} \\ 1 \end{Bmatrix}$

transmission coefficients from the values of $\mathbf{X}_0^-$. A successive determination of the Information Vectors is preformed to determine $\mathbf{X}_n^+$ and the hence the transmission coefficients.

B. Definition of propagation operators and numerical implementation

This subsection concerns the definition of matrix operators illustrated in Fig. 2. In the first step, it is necessary to define two operators which express the transfer of Translation matrices, as follows:

$$[\mathbf{\Omega}_{i-1}^+] = \mathcal{T}_i([\mathbf{\Omega}_i^-]), \quad [\mathbf{\Omega}_i^-] = \mathcal{U}_i([\mathbf{\Omega}_i^+]). \tag{12}$$

$\mathcal{T}_i$ expresses the transfer in layer i and $\mathcal{U}_i$ the transfer over the interface i. Note that $\mathcal{T}_i$ only depends on the physical properties of layer i and $\mathcal{U}_i$ only on the interface type. Due to this, these operators can be implemented separately in independent subroutines. $\mathcal{T}$ (respectively, $\mathcal{U}$) is associated with a subroutine whose inputs are $[\mathbf{\Omega}_i^-]$ and the properties of the layer (respectively, the type of interface).

If a rigid backing configuration is considered $[\mathbf{\Omega}_n^-]$ is known. If the termination condition is associated to a semi-infinite medium, $[\mathbf{\Omega}_n^+]$ is known and

$$[\mathbf{\Omega}_n^-] = \mathcal{U}_n([\mathbf{\Omega}_n^+]). \tag{13}$$

$[\mathbf{\Omega}_0^-]$ can then be deduced from

$$[\mathbf{\Omega}_0^-] = \mathcal{U}_0(\mathcal{T}_1(\mathcal{U}_1(\mathcal{T}_2(....(\mathcal{T}_n([\mathbf{\Omega}_n^-])....))))). \tag{14}$$

For step 3, the Information Vector $\mathbf{X}_0^-$ is transferred toward the interface n. Operators are then defined as:

$$\mathbf{X}_i^- = \mathcal{W}_i(\mathbf{X}_{i-1}^+), \quad \mathbf{X}_i^+ = \mathcal{V}_i(\mathbf{X}_i^-). \tag{15}$$

$\mathcal{W}_i$ represents the transfer of the Information Vector in layer i and $\mathcal{V}_i$ is associated to the one at interface i. Hence, $\mathbf{X}_n^+$ can be deduced from $\mathbf{X}_0^-$:

$$\mathbf{X}_n^+ = \mathcal{V}_n(\mathcal{W}_n(\mathcal{V}_{n-1}(...(\mathcal{W}_1(\mathcal{V}_0(\mathbf{X}_0^-)))...))). \tag{16}$$

One important remark is that problems of instability only occur inside the layers and not at the interfaces. Then, a key point is that $\mathcal{T}$ and $\mathcal{W}$ should not be numerically divergent.

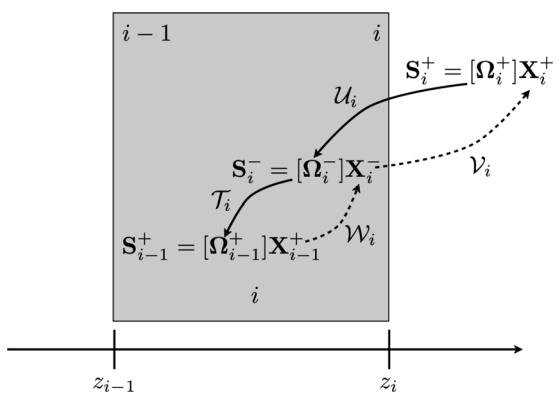

FIG. 2. Transfer of Translation matrices and Information Vectors.

C. Size of the information vector

We are now interested in the comparison of the length of State and Information Vectors. In layer i, in which $2m_i$ waves are travelling, the size of the State Vector is classically of size $2m_i$. One basic remark is that the Transfer Matrix of this layer is determined independently from the other layers. During its numerical derivation, no assumption is made on the links between components of the State Vector: they are considered as independent one from the other. One cause of the divergence of the TMM can then be understood: if a numerical error modifies one component of the State Vector because of finite arithmetics, even in an infinitesimal manner, this error is amplified at the other side of the layer. In the proposed method, the approach is a bit different; the idea is to first consider one side of the panel (the termination condition) and directly expresses the interdependencies on the fields. This has the advantage of reducing the number of needed parameters. Moreover, it can be shown that the size of the Information Vector is equal to m_i. Hence, only the minimal information is transferred thereby reducing the possibility of numerical divergence.

D. Transfer in a layer, $\mathcal{T}$ and $\mathcal{W}$ operators

Reducing the number of unknowns is not sufficient, the method should also control exponentially growing term. In this subsection, expressions of $\mathcal{T}$ and $\mathcal{W}$ are provided as well as a discussion of the stability of the method. Note that this presentation is purely formal and independent of the type of the medium. To simplify notations, index i is omitted in all this subsection. The number of wave in the medium is denoted m, the thickness of the layer by d. Hence, $\mathbf{X}^+$ and $\mathbf{X}^-$ will refer to $\mathbf{X}_{i-1}^+$ and $\mathbf{X}_i^-$ (the same notation is considered for the State Vector $\mathbf{S}$).

The $2m$ eigenvalues of $[\boldsymbol{\alpha}]$ in expression (6) can be numbered in decreasing order of real part

$$\mathrm{Re}(\lambda_1) > \mathrm{Re}(\lambda_2) > \ .. \ > \mathrm{Re}(\lambda_{2m}). \tag{17}$$

The first m eigenvalues have positive real part and the last m have negative real part. Wave vectors are ordered similarly. $\mathbf{\Phi}_k$ denotes the k^{th} column of the eigenvector matrix and let $\mathbf{\Psi}_k$ be the k^{th} row of $[\mathbf{\Psi}] = [\mathbf{\Phi}]^{-1}$. The Transfer Matrix (6) can then be written as the sum of $2m$ matrices:

$$[\mathbf{M}] = \sum_{k=1}^{2m} e^{\lambda_k d}\mathbf{\Phi}_k\mathbf{\Psi}_k. \tag{18}$$

The main idea of the method is to isolate the first $m-1$ terms. $[\mathbf{\Phi}]$ and $[\mathbf{\Psi}]$ are then split into:

$$[\mathbf{\Phi}] = [\mathbf{\Phi}_1...\mathbf{\Phi}_{m-1}|[\mathbf{\Phi}_r]], \quad [\mathbf{\Psi}] = \begin{bmatrix} \mathbf{\Psi}_1 \\ \vdots \\ \mathbf{\Psi}_{m-1} \\ \hline [\mathbf{\Psi}_r] \end{bmatrix}. \tag{19}$$

$[\mathbf{\Phi}_r]$ and $[\mathbf{\Psi}_r]$, respectively, correspond to the $m+1$ last columns (respectively, rows) of $[\mathbf{\Phi}]$ (respectively, $[\mathbf{\Psi}]$). The Transfer Matrix in Eq. (18) now becomes

$$[\mathbf{M}] = \sum_{k=1}^{m-1} e^{\lambda_k d}\boldsymbol{\Phi}_k\boldsymbol{\Psi}_k + e^{\lambda_m d}[\boldsymbol{\alpha}'], \tag{20}$$

where

$$[\boldsymbol{\alpha}'] = [\boldsymbol{\Phi}_r]\begin{bmatrix} 1 & & \\ & e^{(\lambda_{m+1}-\lambda_m)d} & \\ & & \ddots \\ & & e^{(\lambda_{2m}-\lambda_m)d} \end{bmatrix}[\boldsymbol{\Psi}_r]. \tag{21}$$

This separation is of utmost importance. It can be observed that the real part of exponential arguments in $[\boldsymbol{\alpha}']$ is all negative.

Once the decomposition of the Transfer Matrix is done, an adequate choice of $\mathbf{X}^+$ remains. $\mathbf{S}^+$ is now written as:

$$\begin{aligned}\mathbf{S}^+ &= [\mathbf{M}][\boldsymbol{\Omega}^-]\mathbf{X}^- \\ &= \left(\sum_{k=1}^{m-1} e^{\lambda_k d}\boldsymbol{\Phi}_k\boldsymbol{\Psi}_k[\boldsymbol{\Omega}^-] + e^{\lambda_m d}[\boldsymbol{\alpha}'][\boldsymbol{\Omega}^-]\right)\mathbf{X}^-.\end{aligned} \tag{22}$$

Exponential terms in the first part of this expression can formally be integrated in $\mathbf{X}^+$

$$\mathbf{X}^+ = \begin{bmatrix} e^{\lambda_1 d} & & & \\ & \ddots & & \\ & & e^{\lambda_{m-1}d} & \\ & & & e^{\lambda_m d} \end{bmatrix} \underbrace{\begin{bmatrix} \boldsymbol{\Psi}_1[\boldsymbol{\Omega}^-] \\ \vdots \\ \frac{\boldsymbol{\Psi}_{m-1}[\boldsymbol{\Omega}^-]}{\boldsymbol{\Psi}_m[\boldsymbol{\Omega}^-]} \end{bmatrix}}_{[\boldsymbol{\Xi}']} \mathbf{X}^-. \tag{23}$$

As the $\boldsymbol{\Psi}_k$ vectors are linearly independent and $[\boldsymbol{\Omega}^-]$ is associated to independent fields, $[\boldsymbol{\Xi}']$ is invertible. $[\boldsymbol{\Xi}']$ can then be interpreted as the projection of the Translation Matrix on the m leading eigenvectors. Relation (23), including exponentially growing terms, is only an intermediate result and will not be evaluated in the numerical code. The only relation needed between Information Vector is its reciprocal

$$\mathbf{X}^- = \mathcal{W}(\mathbf{X}^+) = [\boldsymbol{\Xi}']^{-1}\begin{bmatrix} e^{-\lambda_1 d} & & & \\ & \ddots & & \\ & & e^{-\lambda_{m-1}d} & \\ & & & e^{-\lambda_m d} \end{bmatrix}\mathbf{X}^+. \tag{24}$$

This relation is numerically stable. Moreover, as $[\boldsymbol{\Xi}']$ is of reduce size, its inversion is obtained using Cramer formulas which are numerically exact.

The real interest of the choice in Eq. (23) for $\mathbf{X}^+$ is that Eq. (24) can be inserted in Eq. (22) to control exponential growing terms:

$$\begin{aligned}\mathbf{S}^+ = &\sum_{k=1}^{m-1}\boldsymbol{\Phi}_k X_k^+ \\ &+ [\boldsymbol{\alpha}'][\boldsymbol{\Omega}^-][\boldsymbol{\Xi}']^{-1}\begin{bmatrix} e^{(\lambda_m-\lambda_1)d} & & & \\ & \ddots & & \\ & & e^{(\lambda_m-\lambda_{m-1})d} & \\ & & & 1 \end{bmatrix}\mathbf{X}^+.\end{aligned} \tag{25}$$

It is observed that no exponential terms exist in the sum and that the remaining part does not contain exponentially growing terms. This form is also similar to that Eq. (9) and provides the expression of $\mathcal{T}$:

$$\begin{aligned}[\boldsymbol{\Omega}^+] = \mathcal{T}[\boldsymbol{\Omega}^-] = &[\boldsymbol{\Phi}_1|...|\boldsymbol{\Phi}_{m-1}|\mathbf{0}] \\ &+ [\boldsymbol{\alpha}'][\boldsymbol{\Omega}^-][\boldsymbol{\Xi}']^{-1}\begin{bmatrix} e^{(\lambda_m-\lambda_1)d} & & & \\ & \ddots & & \\ & & e^{(\lambda_m-\lambda_{m-1})d} & \\ & & & 1 \end{bmatrix}.\end{aligned} \tag{26}$$

From a mathematical point of view, this method is exact as no simplification is made. The method is stable as expressions (24) and (26) do not involve exponentially growing terms.

E. Interface transfer, $\mathcal{U}$ and $\mathcal{V}$ operators

Interface i is considered to give expressions for $\mathcal{U}$ and $\mathcal{V}$. As in the previous subsection, index i will be omitted for simplification. Exponent + (respectively, –) will refer to medium i (respectively, $i-1$). Three types of interfaces should be considered separately dependent on the number of waves in the media on both sides of the interface. For the interfaces considered in Sec. IV, a summary of these relations is given in Table IV.

TABLE IV. Relations between State Vectors at interfaces between different media.

Interface	Elastic solid-PEM	Elastic solid-fluid	PEM-fluid
Numb. waves	$m^- = 2/m^+ = 3$	$m^- = 2/m^+ = 1$	$m^- = 3/m^+ = 1$
Continuity relations	$u_z^e = u_z^t$	$u_z^e = u_z^f$	$u_z^t = u_z^f$
	$u_x^e = u_x^s$	$\sigma_{zz}^e = -p^f$	$p = p^f$
	$\sigma_{zz}^e = \hat{\sigma}_{zz} - p$		
	$\sigma_{xz}^e = \hat{\sigma}_{xz}$		
Dirichlet conditions	$0 = u_z^s - u_z^t$	$\sigma_{xz}^e = 0$	$\hat{\sigma}_{xz} = 0$
			$\hat{\sigma}_{zz} = 0$
Unknowns	$? = p$	$u_x^e = ?$	$u_x^s = ?$
			$u_z^s = ?$

The first case corresponds to media of the same physical type in which $m^- = m^+$. State Vectors at both sides of the interface are linked by $2m^+$ continuity relations for displacements and stresses which are written as

$$\mathbf{S}^- = [\mathbf{T}]\mathbf{S}^+. \tag{27}$$

$[\mathbf{T}]$ is a square interface matrix of size $2m^+$. Note that for continuous fields, $[\mathbf{T}]$ is equal to the identity matrix $[\mathbf{I}_{2m^+}]$. For this case, derivations of $\mathcal{U}$ and $\mathcal{V}$ are straightforward:

$$\mathcal{U}([\mathbf{\Omega}^+]) = [\mathbf{T}][\mathbf{\Omega}^+], \quad \mathcal{V}(\mathbf{X}^-) = \mathbf{X}^-. \tag{28}$$

The second case is associated with interfaces for which $m^- < m^+$. In this case, only $2m^-$ continuity relations on displacements and stress can be written. They are completed by $m^+ - m^-$ Dirichlet conditions on components of $\mathbf{S}^+$. These two relations can be written as:

$$[\mathbf{D}^+]\mathbf{S}^+ = \mathbf{0}, \quad \mathbf{S}^- = [\mathbf{D}^-]\mathbf{S}^+. \tag{29}$$

$[\mathbf{D}^+]$ is a $(m^+ - m^-) \times (2m^+)$ matrix associated to the Dirichlet relations and $[\mathbf{D}^-]$ is a $(2m)^- \times (2m^+)$ matrix associated to the continuity relations. For this type of interface, the simplest and proposed choice for $\mathbf{X}^-$ is to keep the first m^- components of $\mathbf{X}^+$:

$$\mathbf{X}^- = \mathbf{X}^+(1, m^-). \tag{30}$$

The Dirichlet conditions allow to express the remaining components of $\mathbf{X}^+$ from the kept ones:

$$\mathbf{X}^+(m^- + 1, m^+) = [\boldsymbol{\tau}]\mathbf{X}^-, \tag{31}$$

with

$$[\boldsymbol{\tau}] = -\left([\mathbf{D}^+][\mathbf{\Omega}^+(:; m^- + 1 : m^+)]\right)^{-1}[\mathbf{D}^+][\mathbf{\Omega}^+(:; 1 : m^-)]. \tag{32}$$

The colon symbol ":" is associated to the whole range of rows or columns. Expressions for $\mathcal{U}$ and $\mathcal{V}$ are written as:

$$\mathcal{U}([\mathbf{\Omega}^+]) = [\mathbf{D}^-]\left([\mathbf{\Omega}^+(:; 1 : m^-)] + [\mathbf{\Omega}^+(:; m^- + 1 : m^+)][\boldsymbol{\tau}]\right) \tag{33}$$

$$\mathcal{V}(\mathbf{X}^-) = \begin{bmatrix} [\mathbf{I}_{m^-}] \\ [\boldsymbol{\tau}] \end{bmatrix}\mathbf{X}^-. \tag{34}$$

The last type of interface is associated to medium for which $m^- > m^+$. In this case, the components of $\mathbf{S}^-$ can be subdivided in three sets: one associated to fields in $\mathbf{S}^+$, another to the unknown fields and the last one equal to zero. An accurate choice for $\mathbf{X}^-$ is to add the $(m^+ - m^-)$ unknown components $\mathbf{X}'$ to the Information Vector $\mathbf{X}^-$.

$$\mathbf{X}^- = \begin{Bmatrix} \mathbf{X}^+ \\ \hline \mathbf{X}' \end{Bmatrix}. \tag{35}$$

The derivation of $\mathcal{V}$ is then straightforward:

$$\mathbf{X}^+ = \mathcal{V}(\mathbf{X}^-) = \begin{bmatrix} [\mathbf{I}_{n^+}] \\ \hline [\mathbf{0}] \end{bmatrix}\mathbf{X}^-. \tag{36}$$

Finally $\mathcal{U}$ can be written on the form:

$$\mathcal{U}([\mathbf{\Omega}^+]) = [[\mathbf{D}_1][\mathbf{\Omega}^+]|[\mathbf{D}_2]]. \tag{37}$$

$[\mathbf{D}_1]$ is a matrix of dimension $(2m^-) \times (2m^+)$ and expresses the relations between the components of continuous fields of $\mathbf{S}^+$ and $\mathbf{S}^-$. $[\mathbf{D}_2]$ is a Boolean matrix of dimension $(2m^-) \times (m^- - m^+)$ in which the rows are associated to the unknown components $\mathbf{X}'$.

IV. EXAMPLES

A. Acoustic ceiling

The first example is a commonly used suspended acoustical ceiling which illustrates the ability of the technique to model multicomponent panels and rigid backing configurations. The panel consists of three layers: a resistive screen of Material B. modeled with the limp model (layer 1), a porous material with elastic frame of Material A (layer 2) and an air cavity of 10 cm (layer 3) in front of a rigid backing (Table V). The proposed approach is compared to a classical TMM approach calculated by the Maine3A© software for an angle of incidence of 45°. $[\mathbf{\Omega}_3^-]$ is given in the first column of Table II and $[\mathbf{\Omega}_0^-]$ derived from Eq. (14). In this expression, the $\mathcal{U}_i$ and $\mathcal{T}_i$ operators are derived from the expressions

TABLE V. Material properties.

Param.	Unit	Mat. A	Mat. B	Mat. C	Mat. D.	Mat. E	Mat. F	Mat. G	Mat. H
ϕ	[1]	0.95	0.9	0.98				0.98	
σ	(Nsm^{-4})	2 850	2×10^6	15×10^3				1×10^4	
α_∞	[1]	1.05	1.00	1.05				1.0	
Λ	(μm)	300	30	100				150	
Λ'	(μm)	900	100	300				350	
ρ_1	(kgm^{-3})	30.9	120	25	2786	5000	2600	30	900
E	(MPa)	0.22	10	0.14	73300	0.148	2.5×10^4	0.02	5×10^3
ν	[1]	0.25	0	0.3	0.34	0.22	0.3	0	0.3
η_s	[1]	0.12	0.05	0.1	0	0	0.02	0.05	0.05
d	(cm)	3	0.05	2	0.05	0.05	10	5	2

TABLE VI. Links between the operator considered to model acoustic ceiling case and appendices.

Operator	Appendix
$\mathcal{T}_3$	A 3
$\mathcal{U}_2$	B 2
$\mathcal{T}_2$	A 1
$\mathcal{U}_1$	B 1
$\mathcal{T}_1$	A 3
$\mathcal{U}_0$	$\varnothing$

given in subsections III E and III D. For each layer or interface, the operators are determined with particular expressions given in Appendices A and B. Table VI indicates which subsection of these appendices are needed for $\mathcal{U}_i$ and $\mathcal{T}_i$ operators. Real and imaginary parts of the reflection coefficient are presented in Fig. 3 calculated with the proposed approach and the software. A perfect agreement is observed between the proposed approach and the TMM calculation which verifies the validity of the approach. In this case, no divergence of the TMM is observed as the chosen frequency range corresponds to this type of building acoustics problem.

B. Double wall

The second example is the transmission through a double wall construction with a poroelastic layer in between. The panel then consists of three layers: a concrete wall (Material F), a natural fibrous material (Material G), and a wooden wall (Mat. H). Both walls are modeled as elastic solids. The excitation is close to grazing incidence (85°) and the frequency range correspond to the audible frequency range (20 Hz; 20 kHz). Step 3 is in this problem necessary after step 0-2 to deduce the transmission coefficient. A perfect agreement is observed on Fig. 4 between the proposed approach and the TMM below 1.5 kHz where the TMM becomes unstable contrary to the proposed approach. The method derived in this paper was also compared to an analytical model which was specially implemented on this case.

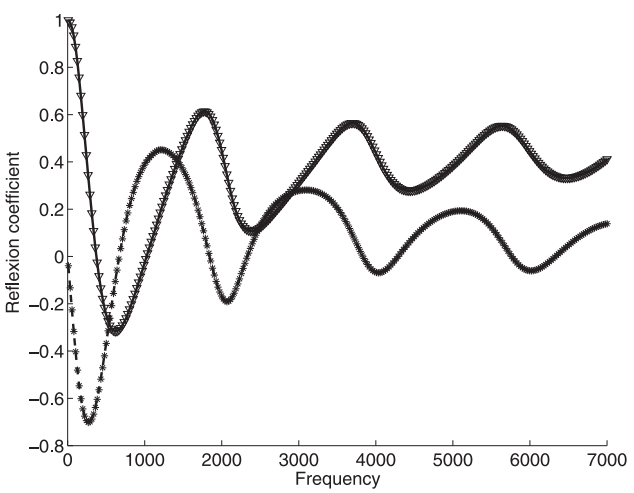

FIG. 3. Acoustic Ceiling. ∇: Maine3A real part; *:Maine3A imaginary part; Solid line: Proposed method real part; Dashed line: Proposed method imaginary part.

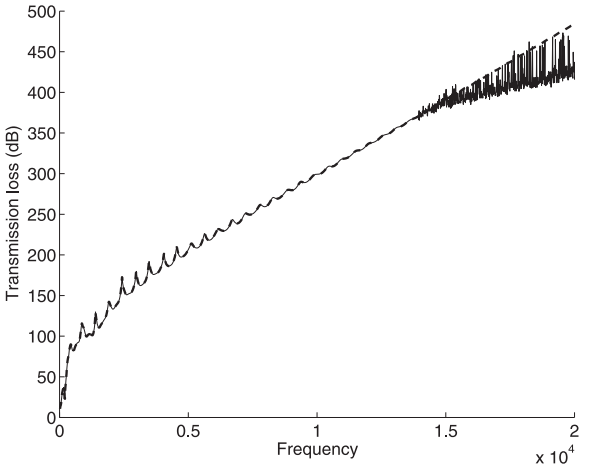

FIG. 4. Transmission loss of a double wall. TMM: Solid line: Proposed method; Dashed line.

The solution of this problem can be derived from a 16 *dof* problem associated to the amplitudes of the waves in the several media as well as the unknown reflexion and transmission coefficient. Origin for the amplitudes of these waves has been chosen at the origin of the interfaces so as not to have numerical discrepancies in the solution. A 16×16 linear system can be obtained from the 16 boundary relations and solved to obtain the reference solution. An exact agreement with the proposed approach is observed below 100 GHz which was chosen as a maximum. Even if there is no physical meaning to test the method up to this frequency, the test indicates the robustness of the proposed approach.

C. Composite material

The last example is the transmission coefficient of a composite multilayered material. The material is the superposition of a glass and an aluminum plate of 0.5 mm (called configuration A). The incident medium is water. The interfaces operators are given in Annexes B 5 and B 6 and the transfer operators are presented in Annex A 2. Transmission

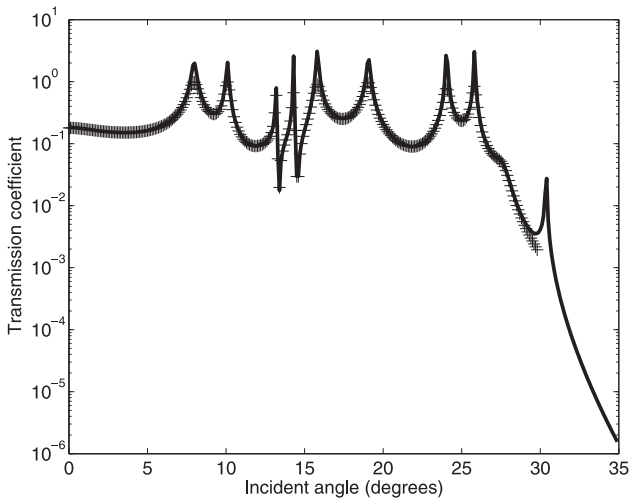

FIG. 5. Modulus of the transmission coefficient of configuration A versus angle of incidence ($f = 1\,MHz$). "+" Floquet method;[15] "Solid line": proposed method.

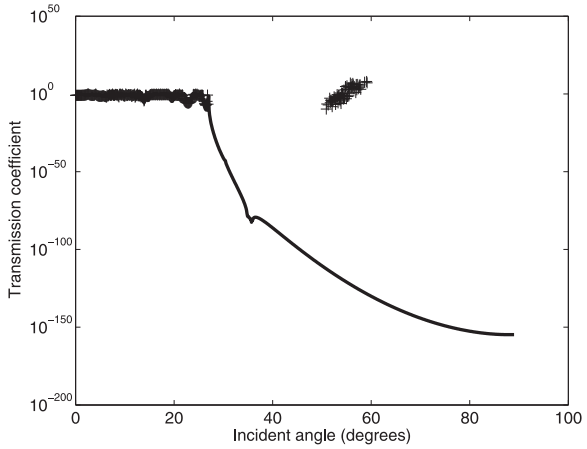

FIG. 6. Modulus of the transmission coefficient of config. B versus angle of incidence ($f=1\,M$Hz). "+" Floquet method;[15] "Solid line": proposed method.

coefficient is presented Fig. 5 at 1 MHz and various angles of incidence. The classical TMM presents divergence for angles larger than 30° because of the existence of evanescent waves. The proposed approach perfectly fits with the TMM before it diverges and is stable for any incidence. The results are shown in Fig. 6 for a multilayer material with 20 layers corresponding to 10 periods of the previous material (called configuration B). Very weak values of the transmission coefficient for angles larger than 30° also illustrate that this problem is an extreme case. It is remarkable that the proposed approach does not become unstable for such problem.

V. CONCLUSION

A recursive approach was presented in this paper to determine the acoustic reflection and transmission coefficients of multilayered panels. Contrary to the Transfer Matrix Method, this new method is not divergent in the case of dissipative materials or when waves are evanescent. Instead of transferring the State Vector in the layer, the principle of this method consists in transferring a so-called Information Vector. This method was shown to be general and mathematically equivalent to the Transfer Matrix Method. It has been illustrated on three different cases associated to classical acoustical problems. Even though only mechanical examples were presented in this paper, this method can be extended to any physical problem of multilayered structures.

APPENDIX A: $\mathcal{T}$ AND $\mathcal{W}$ OPERATORS

This appendix provides the expressions necessary to compute $\mathcal{T}$ and $\mathcal{W}$ operators following the methodology of Sec. III D for three different media. These operators are obtained from the eigenvalues $[\boldsymbol{\lambda}]$ and eigenvectors $[\boldsymbol{\Phi}]$, whose analytical expressions are given. $[\boldsymbol{\Psi}]$ is deduced from $[\boldsymbol{\Phi}]$ with a numerical inversion. In this appendix, matrices are not reordered following the criteria (17). For clarity, $[\boldsymbol{\alpha}]$ is also given together with the constitutive laws and motion equations deduced from the physical models. To shorten expressions, the index i denoting the layer is omitted in this appendix.

1. Poroelastic material

The PEM is modeled with the $\{\mathbf{u}^s, \mathbf{u}^t\}$ representation and notation according to Ref. 6 which is the simplest way to express the full Biot theory with the shortest expressions. This representation yields two motion equations

$$\begin{aligned} \hat{\sigma}_{ij,j} &= -\omega^2 \tilde{\rho}_s u_i^s - \omega^2 \tilde{\rho}_{eq} \tilde{\gamma} u_i^t, \\ -p_{,i} &= -\omega^2 \tilde{\rho}_{eq} \tilde{\gamma} u_i^s - \omega^2 \tilde{\rho}_{eq} u_i^t \end{aligned} \tag{A1}$$

and two constitutive laws:

$$\hat{\sigma}_{ij} = \hat{A}\, \nabla.\mathbf{u}^s\, \delta_{ij} + 2N\varepsilon_{ij}, \quad p = -\tilde{K}_{eq}\, \nabla.\mathbf{u}^t. \tag{A2}$$

Expressions for equivalent densities and elastic coefficients can be found in Refs. 5, 6, and 11. Combining these relations, the expression of $\boldsymbol{\alpha}$ is obtained:

$$[\boldsymbol{\alpha}] = \left[\begin{array}{ccc|ccc} 0 & 0 & 0 & jk_x \dfrac{\hat{A}}{\hat{P}} & \tilde{\gamma} jk_x & -\dfrac{\hat{A}^2 - \hat{P}^2}{\hat{P}} k_x^2 - \tilde{\rho}\omega^2 \\ 0 & 0 & 0 & \dfrac{1}{\hat{P}} & 0 & jk_x \dfrac{\hat{A}}{\hat{P}} \\ 0 & 0 & 0 & 0 & -\dfrac{1}{\tilde{K}_{eq}} + \dfrac{k_x^2}{\tilde{\rho}_{eq}\omega^2} & -jk_x\tilde{\gamma} \\ \hline jk_x & -\tilde{\rho}_s\omega^2 & -\tilde{\rho}_{eq}\tilde{\gamma}\omega^2 & 0 & 0 & 0 \\ 0 & \tilde{\rho}_{eq}\tilde{\gamma}\omega^2 & \tilde{\rho}_{eq}\omega^2 & 0 & 0 & 0 \\ \dfrac{1}{N} & jk_x & 0 & 0 & 0 & 0 \end{array}\right].$$

The eigenvalues of $[\boldsymbol{\alpha}]$ is deduced from the wave numbers of the Biot waves δ_i.[6]

$$[\boldsymbol{\lambda}] = \mathrm{diag}\left[j\sqrt{\delta_1^2 - k_x^2}, -j\sqrt{\delta_1^2 - k_x^2}, j\sqrt{\delta_2^2 - k_x^2}, -j\sqrt{\delta_2^2 - k_x^2}, j\sqrt{\delta_3^2 - k_x^2}, -j\sqrt{\delta_3^2 - k_x^2} \right],$$

wherein δ_1 and δ_2 are associated to the compressional waves and δ_3 to the shear wave.

The analytical expression of the matrix of eigenvectors reads:

$$[\mathbf{\Phi}] = \left[\begin{array}{c|c|c|c|c|c} -2jN\beta_1 k_x & 2jN\beta_1 k_x & -2jN\beta_2 k_2 & 2jN\beta_2 k_2 & jN(\beta_3^2 - k_x^2) & jN(\beta_3^2 - k_x^2) \\ \beta_1 & -\beta_1 & \beta_2 & -\beta_2 & k_x & k_x \\ \mu_1\beta_1 & -\mu_1\beta_1 & \mu_2\beta_2 & -\mu_2\beta_2 & \mu_3 k_x & \mu_3 k_x \\ \alpha_1 & \alpha_1 & \alpha_2 & \alpha_2 & -\alpha_3 & \alpha_3 \\ j\delta_1^2\tilde{K}_{eq}\mu_1 & j\delta_1^2\tilde{K}_{eq}\mu_1 & j\delta_2^2\tilde{K}_{eq}\mu_2 & j\delta_2^2\tilde{K}_{eq}\mu_2 & 0 & 0 \\ k_x & k_x & k_x & k_x & -\beta_3 & \beta_3 \end{array}\right]. \tag{A3}$$

μ_i represents the ratio of displacements for each wave[6] and one defines $\beta_i = \lambda_i/j$ and

$$\alpha_{1,2} = -j\hat{A}\delta_{1,2} - j\,2N\beta_{1,2}^2, \quad \alpha_3 = j\,2N\beta_3 k_x. \tag{A4}$$

2. Elastic-solid

For an isotropic elastic layer, the partial differential equation are given by the classical elasticity theory:

$$\sigma_{ij} = \lambda\,\nabla.\mathbf{u}\,\delta_{ij} + 2\mu\varepsilon_{ij}, \quad \sigma_{ij,j} = -\omega^2\rho u_i. \tag{A5}$$

λ and μ are the Lamé coefficients and ρ is the density of the medium. Combining these two relations gives:

$$[\boldsymbol{\alpha}] = \left[\begin{array}{cc|cc} 0 & 0 & jk_x\dfrac{\lambda}{\lambda+2\mu} & -\dfrac{\lambda^2-(\lambda+2\mu)^2}{\lambda+2\mu}k_x^2 - \rho\omega^2 \\ 0 & 0 & \dfrac{1}{\lambda+2\mu} & jk_x\dfrac{\lambda}{\lambda+2\mu} \\ \hline jk_x & -\rho\omega^2 & 0 & 0 \\ \dfrac{1}{\mu} & jk_x & 0 & 0 \end{array}\right]. \tag{A6}$$

The eigenvalues of $[\boldsymbol{\alpha}]$ are easily obtained from the wave numbers δ_p and δ_s of the compressional and shear waves as:

$$[\boldsymbol{\lambda}] = \mathrm{diag}\left[j\sqrt{\delta_p^2 - k_x^2}, -j\sqrt{\delta_p^2 - k_x^2}, j\sqrt{\delta_s^2 - k_x^2}, -j\sqrt{\delta_s^2 - k_x^2}\right].$$

The analytical expression for the matrix of eigenvectors is:

$$[\mathbf{\Phi}] = \left[\begin{array}{c|c|c|c} -2j\mu\beta_p k_x & 2j\mu\beta_p k_x & j\mu(\beta_s^2 - k_x^2) & j\mu(\beta_s^2 - k_x^2) \\ \beta_p & -\beta_p & k_x & k_x \\ \alpha_p & \alpha_p & -\alpha_s & \alpha_s \\ k_x & k_x & -\beta_s & \beta_s \end{array}\right], \tag{A7}$$

wherein $\beta = \lambda/j$ and

$$\alpha_p = -j\lambda\delta_p - j\,2\mu\beta_p^2, \quad \alpha_s = j\,2\mu\beta_s k_x. \tag{A8}$$

3. Fluid medium

Fluids can be modelled as perfect fluids, equivalent fluid (rigid frame) or limp model depending on the choice of compressibility K and density ρ. One has:

$$-\omega^2\rho u_i = -p, i, \quad p = -K\,\nabla.\mathbf{u}.$$

This leads to $[\boldsymbol{\alpha}]$:

$$[\boldsymbol{\alpha}] = \left[\begin{array}{c|c} 0 & -\dfrac{1}{K} + \dfrac{k_x^2}{\rho\omega^2} \\ \hline \rho\omega^2 & 0 \end{array}\right]. \tag{A9}$$

The eigenvalues of $[\boldsymbol{\alpha}]$ are obtained straightforward with δ the wave number of the compressional wave:

$$[\boldsymbol{\lambda}] = \mathrm{diag}\left[j\sqrt{\delta^2 - k_x^2}, -j\sqrt{\delta^2 - k_x^2}\right].$$

The analytical expression for the matrix of eigenvectors is:

$$[\mathbf{\Phi}] = \left[\begin{array}{c|c} \lambda/j & jK\delta^2 \\ -\lambda/j & jK\delta^2 \end{array}\right]. \tag{A10}$$

APPENDIX B: INTERFACE OPERATORS $\mathcal{U}$ AND $\mathcal{V}$

This appendix provides the expressions of $\mathcal{U}$ and $\mathcal{V}$ which are associated to the interfaces. Only different types of medium are considered here. Subsections are entitled as follows: the first medium is layer i and the second one is medium $i+1$. In each of them, the expressions of $\mathbf{S}^-$ and $\mathbf{S}^+$ are first given. Second, the expressions of $[\mathbf{D}]$ matrices are provided.

1. Fluid medium—Poroelastic material

$$\mathbf{S}^- = \left\{\begin{array}{c} u_z \\ p \end{array}\right\}, \quad \mathbf{S}^+ = \left\{\begin{array}{c} \hat{\sigma}_{xz} = 0 \\ u_z^s \\ u_z^t \\ \hat{\sigma}_{zz} = 0 \\ p \\ u_x^s \end{array}\right\}. \tag{B1}$$

$$[\mathbf{D}^+] = \left[\begin{array}{ccc|ccc} 1 & 0 & 0 & 0 & 0 & 0 \\ 0 & 0 & 0 & 1 & 0 & 0 \end{array}\right] \tag{B2}$$

$$[\mathbf{D}^-] = \left[\begin{array}{ccc|ccc} 0 & 0 & 1 & 0 & 0 & 0 \\ 0 & 0 & 0 & 0 & 1 & 0 \end{array}\right] \tag{B3}$$

2. Poroelastic material—Fluid medium

$$\mathbf{S}^- = \begin{Bmatrix} \hat{\sigma}_{xz} = 0 \\ u_z^s \\ u_z^a \\ \hat{\sigma}_{zz} = 0 \\ p^a \\ u_x^s \end{Bmatrix}, \quad \mathbf{S}^+ = \begin{Bmatrix} u_z^a \\ p^a \end{Bmatrix} \tag{B4}$$

$$[\mathbf{D}_1] = \left[\begin{array}{c|c} 0 & 0 \\ 0 & 0 \\ 1 & 0 \\ \hline 0 & 0 \\ 0 & 1 \\ 0 & 0 \end{array}\right], \quad [\mathbf{D}_2] = \left[\begin{array}{c|c} 0 & 0 \\ 1 & 0 \\ 0 & 0 \\ \hline 0 & 0 \\ 0 & 0 \\ 0 & 1 \end{array}\right] \tag{B5}$$

3. Equivalent fluid medium—Poroelastic material

$$\mathbf{S}^- = \begin{Bmatrix} u_z \\ p \end{Bmatrix}, \quad \mathbf{S}^+ = \begin{Bmatrix} \hat{\sigma}_{xz} \\ u_z^s = 0 \\ u_z^t \\ \hat{\sigma}_{zz} \\ p \\ u_x^s = 0 \end{Bmatrix}. \tag{B6}$$

$$[\mathbf{D}^+] = \left[\begin{array}{ccc|ccc} 0 & 1 & 0 & 0 & 0 & 0 \\ 0 & 0 & 0 & 0 & 0 & 1 \end{array}\right] \tag{B7}$$

$$[\mathbf{D}^-] = \left[\begin{array}{ccc|ccc} 0 & 0 & 1 & 0 & 0 & 0 \\ 0 & 0 & 0 & 0 & 1 & 0 \end{array}\right] \tag{B8}$$

4. Poroelastic material—Equivalent fluid medium

$$\mathbf{S}^- = \begin{Bmatrix} \hat{\sigma}_{xz} \\ u_z^s = 0 \\ u_z^a \\ \hat{\sigma}_{zz} \\ p^a \\ u_x^s = 0 \end{Bmatrix}, \quad \mathbf{S}^+ = \begin{Bmatrix} u_z^a \\ p^a \end{Bmatrix} \tag{B9}$$

$$[\mathbf{D}_1] = \left[\begin{array}{c|c} 0 & 0 \\ 0 & 0 \\ 1 & 0 \\ \hline 0 & 0 \\ 0 & 1 \\ 0 & 0 \end{array}\right], \quad [\mathbf{D}_2] = \left[\begin{array}{c|c} 1 & 0 \\ 0 & 0 \\ 0 & 0 \\ \hline 0 & 1 \\ 0 & 0 \\ 0 & 0 \end{array}\right] \tag{B10}$$

5. Fluid medium—Elastic medium

$$\mathbf{S}^- = \begin{Bmatrix} u_z \\ p = -\sigma_{zz} \end{Bmatrix}, \quad \mathbf{S}^+(z) = \begin{Bmatrix} \sigma_{xz} = 0 \\ u_z \\ \sigma_{zz} \\ u_x \end{Bmatrix} \tag{B11}$$

$$[\mathbf{D}^+] = \left[\begin{array}{cc|cc} 1 & 0 & 0 & 0 \end{array}\right] \tag{B12}$$

$$[\mathbf{D}^-] = \left[\begin{array}{cc|cc} 0 & 1 & 0 & 0 \\ 0 & 0 & -1 & 0 \end{array}\right] \tag{B13}$$

6. Elastic medium— Fluid medium

$$\mathbf{S}^- = \begin{Bmatrix} \sigma_{xz} = 0 \\ u_z \\ \sigma_{zz} = -p \\ u_x \end{Bmatrix}, \quad \mathbf{S}^+ = \begin{Bmatrix} u_z \\ p \end{Bmatrix} \tag{B14}$$

$$[\mathbf{D}_1] = \left[\begin{array}{c|c} 0 & 0 \\ 1 & 0 \\ \hline 0 & 1 \\ 0 & 0 \end{array}\right], \quad [\mathbf{D}_2] = \left[\begin{array}{c|c} 0 & 0 \\ 0 & 0 \\ \hline 0 & 1 \\ 0 & 0 \end{array}\right] \tag{B15}$$

[1] J. F. Allard and N. Atalla, *Propagation of Sound in Porous Media-Modelling Sound Absorbing Materials* (Wiley, Ltd., London, 2009).
[2] J. F. Allard, O. Dazel, J. Descheemaeker, N. Geebelen, L. Boeckx, and W. Lauriks, J. Appl. Phys. **106**, 014906 (2009).
[3] B. Brouard, D. Lafarge, and J. F. Allard, J. Sound Vib. **183**, 129 (1995).
[4] M. Castaings and B. Hosten, J. Acoust. Soc. Am. **95**, 1931 (1994).
[5] O. Dazel, B. Brouard, N. Dauchez, and A. Geslain, Acta. Acust. Acust. **95**, 527 (2009).
[6] O. Dazel, B. Brouard, C. Depollier, and S. Griffiths, J. Acoust. Soc. Am. **121**, 3509 (2007).
[7] N. Haskell, Bull. Seismol. Soc. Am. **43**, 17 (1953).
[8] B. Hosten and M. Castaings, J. Acoust. Soc. Am. **94**, 1488 (1993).
[9] J. Jocker, D. Smeulders, G. Drijkoningen, C. van der Lee, and A. Kalfsbeek, Geophys. **69**, 1071, doi:10.1190/1.1778249 (2004).
[10] B. Kennett and N. Kerry, Geophys. J. R. Astron. Soc. **57**, 557 (1979).
[11] P. Khurana, L. Boeckx, W. Lauriks, P. Leclaire, O. Dazel, and J. F. Allard, J. Acoust. Soc. Am. **125**, 915 (2009).
[12] L. Knopoff, Bull. Seismol. Soc. Am **54**, 431 (1964).
[13] C.-M. Krowne, IEEE Trans. Antennas Propag. **34**, 247 (1986).
[14] M. Lowe, IEEE Trans. Ultrason. Ferroelectr. Freq. Control **42**, 525 (1995).
[15] C. Potel and J. de Belleval, J. Acoust. Soc. Am. **93**, 2669 (1993).
[16] C. Potel and J. De Belleval, J. Appl. Phys. **74**, 2208 (1993).
[17] S. Pride, E. Tromeur, and J. Berryman, Geophys. **67**, 271, doi:10.1190/1.1451799 (2002).
[18] D. Rhazi and N. Atalla, J. Acoust. Soc. Am.**127**, EL30 (2010).
[19] S. I. Rokhlin and L. Wang, J. Acoust. Soc. Am. **112**, 822 (2002).
[20] W. Thomson, J. Appl. Phys. **21**, 89 (1950).
[21] J.-L. Tsalamengas, IEEE Trans. Antennas Propag. **37**, 1582 (1989).
[22] J.-L. Tsalamengas, IEEE Trans. Antennas Propag. **38**, 9 (1990).
[23] H. Yang, IEEE Trans. Microwave Theory Tech. **43**, 1626 (1995).
[24] H. Yang, IEEE Trans. Antennas Propag. **45**, 520 (1997).